ACS APPLIED MATERIALS & INTERFACES

Letter

www.acsami.org

Efficient n-GaAs Photoelectrodes Grown by Close-Spaced Vapor Transport from a Solid Source

Andrew J. Ritenour, Richard C. Cramer, Solomon Levinrad, and Shannon W. Boettcher*

Department of Chemistry and the Materials Science Institute, University of Oregon, University of Oregon, Eugene, Oregon 97403, United States

Supporting Information

ABSTRACT: n-GaAs films were grown epitaxially on n^+-GaAs substrates by a close-spaced vapor transport method and their photoelectrochemical energy conversion properties studied. Under 100 mW cm^{-2} of ELH solar simulation, conversion efficiencies up to 9.3% for CSVT n-GaAs photoanodes were measured in an unoptimized ferrocene/ferrocenium test cell. This value was significantly higher than the 5.7% measured for similarly doped commercial n-GaAs wafers. Spectral response experiments showed that the higher performance of CSVT n-GaAs films relative to the commercial wafers was due to longer minority carrier diffusion lengths (L_D), up to 1,020 nm in the CSVT films compared to 260 nm in the commercial n-GaAs wafers. Routes to improve the performance of CSVT GaAs and the implications of these results for the development of scalable GaAs-based solar energy conversion devices are discussed.

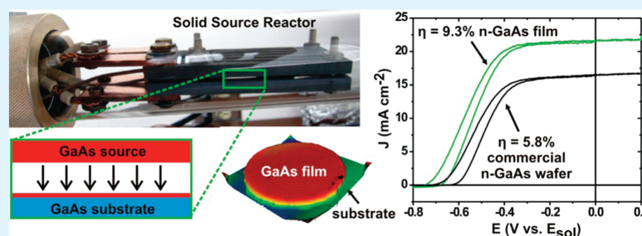

KEYWORDS: *solar energy, gallium arsenide, close-spaced vapor transport, photoelectrochemistry*

The excellent optoelectronic properties of GaAs make it an attractive material for solar energy conversion.[1,2] It has a high optical absorption coefficient, absorbing >98% of above band gap photons within 1 μm of film thickness.[3] It has an ideal direct band gap of 1.42 eV for solar energy conversion which can also be tuned by alloying with Al or P for multijunction photovoltaic (PV) or photoelectrochemical (PEC) applications.[4] Indeed, GaAs is used to make the most efficient single-junction PV known, with recent champion cells achieving 27.6% efficiency under standard one-sun test conditions.[5] Unfortunately, the scalability of GaAs photovoltaics is limited by the high cost of metal–organic chemical vapor deposition (MOCVD), which employs toxic and pyrophoric gas-phase precursors.[2] Low-cost routes to high-quality GaAs are needed.

Close-space vapor transport (CSVT) is an alternative technique for depositing GaAs that uses bulk GaAs as the only precursor.[6] The use of a solid precursor circumvents challenges associated with the handling of toxic and pyrophoric gas-phase starting materials. The CSVT reactor consists of a bulk GaAs source and a planar substrate sandwiched between graphite blocks and separated by a thin quartz spacer (Figure 1). The entire assembly is enclosed in a quartz tube (see Figure S1 in the Supporting Information). The source is heated in a reducing atmosphere (hydrogen or forming gas) containing water vapor as a transport agent. The water reacts with the GaAs source to produce the volatile species as shown in Scheme 1.[7−9]

The temperature gradient between the heated GaAs source and the cooler substrate provides a driving force for vapor transport of GaAs. Diffusion of the gas-phase reactants through

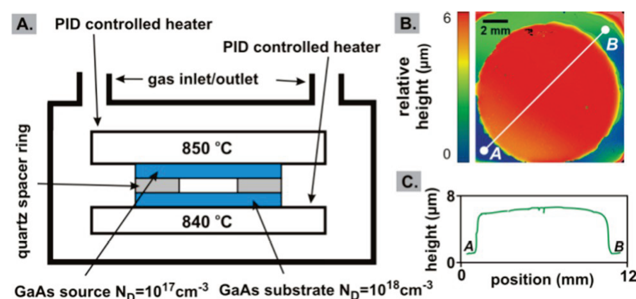

Figure 1. (A) CSVT reactor schematic. Wires for the thermocouples and graphite resistive heaters are omitted for clarity. (B) Color-relief topographical image of the wafer surface after film growth obtained using optical profilometry. The shape of the film is a result of the circular quartz spacer. (C) Height profile of the line AB shown in (B).

Scheme 1. Vapor Transport of GaAs Facilitated by Water Vapor

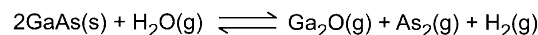

$$2GaAs(s) + H_2O(g) \rightleftharpoons Ga_2O(g) + As_2(g) + H_2(g)$$

the temperature gradient results in supersaturation at the cooler substrate surface, causing As_2, Ga_2O, and H_2 to decompose into GaAs and H_2O. The process is carried out at atmospheric pressure, which allows for growth rates up to 1 μm min^{-1} with ca. 95% yield.[6] The overall deposition process and apparatus

Received: November 21, 2011
Accepted: December 3, 2011
Published: December 3, 2011

© 2011 American Chemical Society

Table 1. Electrode Parameters for *n*-GaAs Photoanodes

sample	thickness (μm)	[H_2O] (ppm)	V_{OC} (V)	J_{SC} (mA cm^{-2})	η (%)	ff	η_{corr} (%)	ff$_{corr}$	L_D (nm)	$J_{SC,AM1.5CALC}$ (mA cm^{-2})
CSVT film	5.5	1,700	−0.72	21.6	9.3	0.59	12.8	0.72	1,020	18.7
CSVT film	3.7	430	−0.69	18.6	7.3	0.57	9.1	0.71	730	17.7
CSVT film	1.3	170	−0.69	18.2	7.8	0.62	9.2	0.74	550	16.3
CSVT film	2.8	20	−0.67	17.5	5.8	0.49	8.1	0.69	300	14.7
n-GaAs wafer	N/A	N/A	−0.71	17.6	5.8	0.47	7.6	0.60	260	13.7
n^+-GaAs wafer	N/A	N/A	−0.60	12.1	3.9	0.49	5.2	0.67	180	10.7

are similar to the vapor-transport process used commercially for the high-throughput/low-cost growth of CdTe thin-film photovoltaics.[10,11] CSVT is therefore a potentially scalable cost-effective route to GaAs thin films.[12−15]

Despite the advantages of CSVT, its use for optoelectronic devices remains limited. Since its initial development in 1963, epitaxial films of GaAs have been grown by CSVT on GaAs, Ge, and Si.[6,16] Electrical properties of these films such as dopant density ($N_D = 1 \times 10^{16}$ to 1×10^{17} cm^{-3}), mobility (μ_e = 3000−4200 cm^2 V^{-1} s^{-1}), and photoluminescence (PL) intensity have been measured and indicate that CSVT GaAs films may be suitable for solar-energy conversion.[17−19] However, the only reported PV device fabricated using CSVT GaAs was that of Mauk and co-workers; an Au-GaAs-on-Si Schottky barrier PV which yielded a short-circuit current density of 7 mA cm^{-2} under one sun of solar simulation (no open-circuit-voltage/efficiency was reported).[20] A key question is whether or not it is possible to achieve sufficient performance using CSVT GaAs to motivate the further development of more complicated device architectures.[16,17]

To evaluate this possibility, we grew *n*-GaAs thin films with varying concentration of water vapor, [H_2O], and measured their PEC energy conversion properties. The PEC characterization approach enabled measurement of standard PV device parameters including short-circuit current densities, spectral response, open-circuit voltages, fill-factors, and conversion efficiencies, without the need to fabricate solid-state p-n junctions, top contact grids, or address other device-related engineering issues.

All films were grown in a home-built CSVT reactor (Figure 1 and Figure S1 in the Supporting Information). A moderately doped ($N_D \sim 10^{17}$ cm^{-3}) *n*-GaAs wafer held at 850 °C was used as the source and a highly doped ($N_D \sim 10^{18}$ cm^{-3}) n^+-GaAs wafer held at 840 °C as the substrate. The films were grown epitaxially on n^+-GaAs substrates in order to isolate any defects associated with the CSVT growth process from those associated with the growth of GaAs on a nonlattice-matched substrate. Observed growth rates were 70−420 nm min^{-1} depending on [H_2O], which was varied from 20−1700 ppm (see Figure S2 in the Supporting Information). Film thicknesses, which ranged from 1.3−5.5 μm (Table 1), were sufficient to ensure that effectively all incident light of energy greater than the GaAs band gap was absorbed in the CSVT film and not in the substrate wafer.

Rectifying contacts were made to *n*-GaAs by immersing it in an electrolyte consisting of 1 M $LiClO_4$, 100 mM ferrocene, and 0.5 mM ferrocenium in dry acetonitrile (see Figure S10 in the Supporting Information). This electrolyte is known to yield reasonable PEC performance for *n*-GaAs.[21,22] 100 mW cm^{-2} of solar simulation was provided by a 300 W ELH lamp. A Pt wire poised at the solution potential was used as a reference electrode and a separate Pt mesh was used as the counter electrode (see Figure S9B in the Supporting Information). The solution was rapidly stirred during measurements to aid mass transport.

Figure 2 shows the current-density versus potential (J−E) data collected for CSVT and control GaAs samples, both before

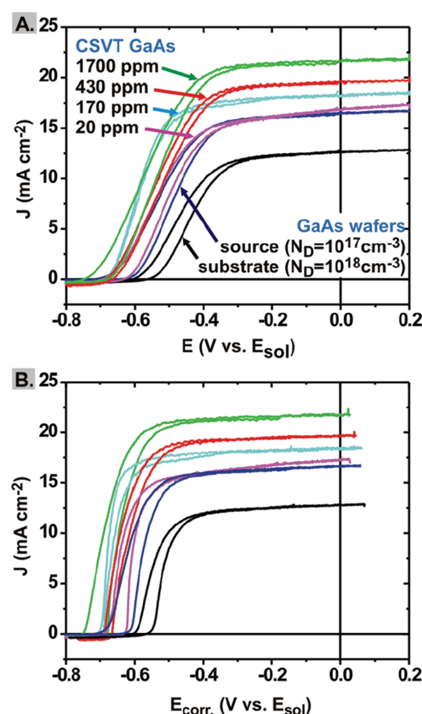

Figure 2. (A) J−E curves obtained from CSVT *n*-GaAs films grown at four different water concentrations and two different control wafers measured under 100 mW cm^{-2} of solar simlulation in ferrocene/ferrocenium/acetonitrile. (B) Same data after correction for solution resistance and concentration overpotential (see eq S2 in the Supporting Information) showing improved fill factors.

and after the typical corrections for solution resistance and concentration overpotential (see eq S2 in the Supporting Information).[23] A summary of electrode parameters for the six representative electrodes shown is provided in Table 1. The complete data set for all 18 electrodes measured is given in Table S1 in the Supporting Information and shows similar trends. The J-E data shows that films grown with higher [H_2O] (and thus at higher growth rates) yield higher current densities, photovoltages, and efficiencies. Interestingly, the CSVT-grown GaAs films are better than the specific commercial *n*-GaAs control wafer, which was also used as a source to grow the CSVT films. The n^+-GaAs control samples (the material which was also used as a substrate for the CSVT films) showed the lowest performance, indicating that the small amount of light absorbed within the substrate (<1% for all films) does not impact the observed performance of the CSVT samples. The lower performance of the *n*-GaAs control electrodes is similar

to that previously measured for untextured photoelectrodes made from commercial *n*-GaAs.[21]

The photocurrent measured for *n*-GaAs photoelectrodes is known to be inversely related to N_D due doping-induced degradation of the minority carrier diffusion length, L_D,[21] but capacitance−voltage studies showed there was no significant or systematic difference in doping between the series of CSVT GaAs samples. All samples yielded N_D between $1 - 5 \times 10^{17}$ cm^{-3} (see Table S2 in the Supporting Information). Two other possible causes for the observed J_{SC} trend are: (1) differences in reflectivity and (2) changes in carrier collection efficiency that are due to differences in L_D, and associated with other nonradiative defects.

Optical measurements in an integrating sphere were used to show that the reflectivity of the GaAs wafers and CSVT samples were similar and consistent with that predicted for smooth GaAs-air interfaces based on the known optical constants of GaAs (Figure 3).[3] Spectral response measurements, however, showed significant differences between the electrodes (Figure 4). The wavelength dependence of the GaAs absorption coefficient, $\alpha(\lambda)$, causes low-energy photons to be absorbed deeper in the film than high-energy photons. Thus, reduced response for lower energy photons is indicative of a shorter L_D. To quantitatively analyze the spectral response data, the external quantum efficiency (Φ_{ext}) was converted to internal quantum efficiency (Φ_{int}) using the relation:

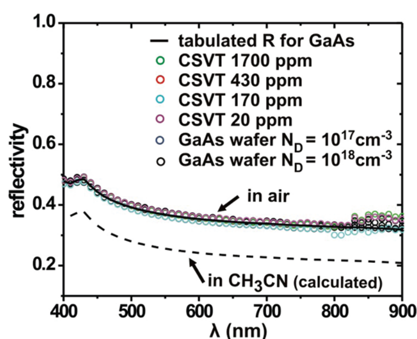

Figure 3. Reflectivity of CSVT GaAs and commercial single crystal GaAs wafers as measured in an integrating sphere. Reflectivity of GaAs in acetonitrile based on the Fresnel equations is also shown.

$$\Phi_{int} = \frac{\Phi_{ext}}{(1 - R_1)(1 - R_2)} \quad (1)$$

where R_1 is the reflectivity of the air/glass interface and R_2 is the reflectivity of the acetonitrile/GaAs interface. R_1 and R_2 were calculated using the Fresnel equation and the known optical constants of GaAs, acetonitrile, glass, and air. The reflectivity of the glass/acetonitrile interface is negligible. The dependence of Φ_{int} on excitation wavelength was fit to the Gärtner model for carrier collection in order to extract L_D according to the relation

$$\Phi_{int} = \left(1 - \frac{e^{-\alpha(\lambda)W}}{1 + \alpha(\lambda)L_D}\right) \quad (2)$$

where W is the depletion layer width, as estimated by capacitance measurements (see the Supporting Information), and the value of $\alpha(\lambda)$ was obtained from tabulated data.[3,24,25] The Gärtner model assumes perfect collection efficiency for carriers generated in the semiconductor depletion region with carrier collection in the quasi-neutral region governed by L_D and has been used to extract diffusion lengths from *n*-GaAs that are identical to those measured directly using electron-beam-induced-current techniques.[26] Consistent with the *J*−*E* curves, the L_D values increased with increasing growth rate and [H_2O], up to 1,020 nm for the best CSVT sample (Table 1). These values compare well with previous measurements on a variety of GaAs single crystals that ranged from 350 to 1200 nm.[26]

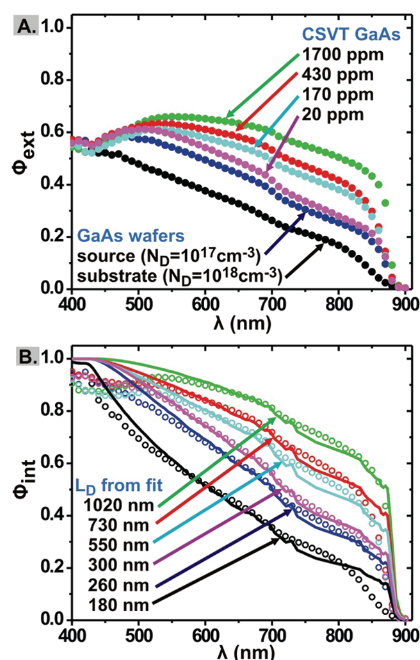

Figure 4. (A) Φ_{ext} plotted versus wavelength for CSVT GaAs thin films and commercial GaAs wafers. These curves are uncorrected for reflectance and solution absorbance (λ_{max} = 440 nm). (B) Φ_{int} for the same electrodes (open circles) and fits (solid lines) based on the Gärtner model. In the calculation of L_D we used data corresponding to wavelengths for which the solution was transparent (500−900 nm).

The observation that GaAs films grown with higher [H_2O] performed better than those grown with low [H_2O] is unexpected. Mimila-Arroyo and co-workers observed that the PL intensity of CSVT GaAs thin films could be improved by reducing [H_2O] during growth to less than 100 ppm and suggested this was related to reduced incorporation of oxygen defects that are known to reduce the minority carrier lifetime in GaAs.[18,27] Increased PL is typically associated with reduced nonradiative recombination that should indicate longer L_D. We note that the films in Mimila-Arroyo's study were deposited using a higher temperature gradient of 80−130 °C, compared to the 10 °C used here. The larger driving force for deposition may have resulted in increased oxygen incorporation relative to the conditions used here. PL experiments are also highly dependent on surface recombination and thus differences in the precise surface chemistry/passivation could be important.[28] Our findings indicate that, under the present growth conditions, defects originating from the water vapor are not limiting carrier collection. Additional work is required to identify and quantify all defects and impurities as a function of growth conditions. Convolution of the spectral response data with the American Society for Testing and Materials Air Mass 1.5 Global spectrum (ASTM AM1.5G) yields photocurrents that were on average 15% lower than those measured under the

dx.doi.org/10.1021/am201631p | ACS Appl. Mater. Interfaces 2012, 4, 69−73

ELH lamp (Table 1). These differences are due to the known differences between lamp spectra and the reference spectra.[29,30]

The results reported here suggest that the electronic quality of CSVT GaAs is sufficient for use in solar energy conversion applications and motivate significant further study. The best CSVT GaAs photoanodes yielded an efficiency of 9.3%, which approaches that achieved in previous studies using the same electrolyte and illumination source with high-quality MOCVD-grown GaAs epi-layers (where up to 11% efficiency was observed).[22] Correction for cell-related solution losses, that could be eliminated in a solid-state cell design, yield corrected efficiencies for the CSVT films near 13% (Table 1).[31] Furthermore, the external quantum efficiency of the CSVT GaAs thin-film devices as well as that of the control wafers could be substantially improved through the use of surface texturing both to decrease reflective losses (~24% of above-bandgap photons for the GaAs/ACN interface) and boost carrier collection via three-dimensional structuring.[25,32] Higher photoanode efficiencies (ca. 15%) for Ru or Os-modified, surface-roughened *n*-GaAs wafers have been obtained in aqueous selenide electrolytes.[33,34] Use of these electrolytes would enable higher absolute efficiencies for CSVT *n*-GaAs as well.

Efforts to passivate the CSVT GaAs surface to increase the photovoltage in PEC cells and to enable applications in PEC water splitting are underway.[35−37] We also note that it should be possible to grow GaAs nanostructures by controlling the nucleation and growth pathways in this simple CSVT reactor without requiring molecular beam epitaxy or MOCVD equipment.[38] Because the use of single-crystal GaAs wafers as growth substrates is prohibitively expensive for practical solar energy conversion applications, we are studying the growth of CSVT GaAs on non-lattice-matched substrates and metal foils.[7,20,39]

■ ASSOCIATED CONTENT

Ⓢ Supporting Information

Descriptions and photos of the CSVT reactor; experimental methods for PEC, spectral response, and capacitance−voltage measurements; film characterization including SEM, XRD, and reflectivity measurements; electrode fabrication procedures. This material is available free of charge via the Internet at http://pubs.acs.org.

■ AUTHOR INFORMATION

Corresponding Author

*E-mail: swb@uoregon.edu.

■ ACKNOWLEDGMENTS

This work was supported by startup funds provided by the University of Oregon. S.L. was supported by the Pete and Rosalie Johnson Summer Internship program. This project made use of equipment in the SUNRISE Photovoltaic Laboratory supported by the Oregon Built Environment and Sustainable Technologies (BEST) signature research center. Assistance from Fuding Lin, Adam Smith, Lena Trotochaud, Kris Johnson, John Boosinger, Cliff Dax, and Michael Mauk is also acknowledged.

■ REFERENCES

(1) Fahrenbruch, A. L.; Bube, R. H. *Fundamentals of Solar Cells: Photovoltaic Solar Energy Conversion*; Academic Press: New York, 1983.

(2) Stringfellow, G. B. *Organometallic Vapor-Phase Epitaxy*; 2nd ed.; Academic Press: New York, 1999.

(3) *Handbook of Optical Constants of Solids*; Palik, E. D., Ed.; Academic Press: New York, 1985.

(4) Adachi, S. *Physical Properties of III−V Semiconductor Compounds*; 1st ed.; John Wiley & Sons: New York, 1992.

(5) Kayes, B. M.; Nie, H.; Twist, R.; Spruytte, S. G.; Reinhardt, F.; Kizilyalli, I. C.; Higashi, G. S. In *PVSC37* 2011.

(6) Nicoll, F. H. *J. Electrochem. Soc.* **1963**, *110*, 1165.

(7) Mauk, M. G.; Feyock, B. W.; Cotter, J. E. *J. Cryst. Growth* **2001**, *225*, 528.

(8) Hammadi, M.; Bourgoin, J. C.; Samic, H. *J. Mater. Sci.—Mater. Electron* **1999**, *10*, 399.

(9) Chavez, F.; Mimila-Arroyo, J.; Bailly, F.; Bourgoin, J. C. *J. Appl. Phys.* **1983**, *54*, 6646.

(10) McCandless, B. E.; Sites, J. R. In *Handbook of Photovoltaic Science and Engineering*; John Wiley & Sons: New York, 2011, p 600.

(11) Birkmire, R. W.; McCandless, B. E. *Curr. Opin. Solid State Mater. Sci.* **2010**, *14*, 139.

(12) Cossement, D.; Dodelet, J. P.; Bretagnon, T.; Jean, A.; Lombos, B. A. *J. Electrochem. Soc.* **1991**, *138*, 830.

(13) Lalande, G.; Guelton, N.; Cossement, D.; Saint-Jacques, R. G.; Dodelet, J. P. *Can. J. Phys.* **1994**, *72*, 225.

(14) Le Bel, C.; Cossement, D.; Dodelet, J. P.; Leonelli, R.; DePuydt, Y.; Bertrand, P. *J. Appl. Phys.* **1993**, *73*, 1288.

(15) Mauk, M. G. *Electronic GaAs-on-Silicon Material for Advanced High-Speed Optoelectronic Devices*; U.S. Army Research Office: Durham, NC, 1991.

(16) Perrier, G.; Philippe, R.; Dodelet, J. P. *J. Mater. Res.* **1988**, *3*, 1031.

(17) Koskiahde, E.; Cossement, D.; Paynter, R.; Dodelet, J. P.; Jean, A.; Lombos, B. A. *Can. J. Phys.* **1989**, *67*, 251.

(18) Mimila-Arroyo, J.; Legros, R.; Bourgoin, J. C.; Chavez, F. *J. Appl. Phys.* **1985**, *58*, 3652.

(19) Lombos, B. A.; Bretagnon, T.; Jean, A.; Le Van Mao, R.; Bourassa, S.; Dodelet, J. P. *J. Appl. Phys.* **1990**, *67*, 1879.

(20) Mauk, M. G.; Feyock, B. W.; Hall, R. B.; Cavanaugh, K. D.; Cotter, J. E. In *Conference Record of the 26th IEEE Photovoltaic Specialists Confernce*; Anaheim, CA, Oct 3, 1997 ; IEEE: Piscatway, NJ, 1997; p 511.

(21) Gronet, C. M.; Lewis, N. S. *Appl. Phys. Lett.* **1983**, *43*, 115.

(22) Casagrande, L. G.; Juang, A.; Lewis, N. S. *J. Phys. Chem. B* **2000**, *104*, 5436.

(23) Boettcher, S. W.; Spurgeon, J. M.; Putnam, M. C.; Warren, E. L.; Turner-Evans, D. B.; Kelzenberg, M. D.; Maiolo, J. R.; Atwater, H. A.; Lewis, N. S. *Science* **2010**, *327*, 185.

(24) Gärtner, W. W. *Phys. Rev.* **1959**, *116*, 84.

(25) Price, M. J.; Maldonado, S. *J. Phys. Chem. C* **2009**, *113*, 11988.

(26) Tufts, B. J.; Abrahams, I. L.; Casagrande, L. G.; Lewis, N. S. *J. Phys. Chem.* **1989**, *93*, 3260.

(27) *Crystal Growth Technology*; Scheel, H. J., Capper, P., Eds.; Wiley-VCH: Weinheim, Germany, 2008.

(28) Skromme, B. J.; Sandroff, C. J.; Yablonovitch, E.; Gmitter, T. *Appl. Phys. Lett.* **1987**, *51*, 2022.

(29) Casagrande, L. G.; Tufts, B. J.; Lewis, N. S. *J. Phys. Chem.* **1991**, *95*, 1373.

(30) Boettcher, S. W.; Warren, E. L.; Putnam, M. C.; Santori, E. A.; Turner-Evans, D.; Kelzenberg, M. D.; Walter, M. G.; McKone, J. R.; Brunschwig, B. S.; Atwater, H. A.; Lewis, N. S. *J. Am. Chem. Soc.* **2011**, *133*, 1216.

(31) Bard, A. J.; Faulkner, L. R. *Electrochemical Methods*, 2nd ed.; John Wiley & Sons: New York, 2001.

(32) Föll, H.; Langa, S.; Carstensen, J.; Christophersen, M.; Tiginyanu, I. M. *Adv. Mater.* **2003**, *15*, 183.

(33) Tufts, B. J.; Abrahams, I. L.; Santangelo, P. G.; Ryba, G. N.; Casagrande, L. G.; Lewis, N. S. *Nature* **1987**, *326*, 861.

(34) Parkinson, B. A.; Heller, A.; Miller, B. *J. Electrochem. Soc.* **1979**, *126*, 954.

(35) Wang, Y.; Darici, Y.; Holloway, P. H. *J. Appl. Phys.* **1992**, 71.

(36) Chen, Y. W.; Prange, J. D.; Dühnen, S.; Park, Y.; Gunji, M.; Chidsey, C. E. D.; McIntyre, P. C. *Nat. Mater.* **2011**, *10*, 539.
(37) Mauk, M. G.; Tata, A. N.; Feyock, B. W. *J. Cryst. Growth* **2001**, *225*, 359.
(38) Rudolph, D.; Hertenberger, S.; Bolte, S.; Paosangthong, W.; Spirkoska, D. e.; Döblinger, M.; Bichler, M.; Finley, J. J.; Abstreiter, G.; Koblmüller, G. *Nano Lett.* **2011**, 3848.
(39) Heller, A.; Miller, B. I.; Chu, S. S.; Lee, Y. T. *J. Am. Chem. Soc.* **1979**, *101*, 7633.